**THE USE OF A REGIONAL CLIMATE- AND WAVE MODEL FOR THE ASSESSMENT OF CHANGES OF THE FUTURE WAVE CLIMATE IN THE WESTERN BALTIC SEA**

Norman Dreier[1], Peter Fröhle[1], Dörte Salecker[1], Christian Schlamkow[2] and Xu Zhenshan[3]

On the basis of hourly simulated wind data from a regional circulation model (Cosmo-CLM) wave conditions from 1960 to 2100 are calculated for two realisations each of the global emission scenarios A1B and B1 using a numerical wave model for the area of the Western Baltic Sea. Comparisons of the 30 years averages of the wave conditions between the future and the past show that the changes of the average wave conditions can be directly linked to the changes of the average wind conditions. The changes of the average wave conditions and extreme wave events are characterised by high spatial and annual variability. In addition the changes depend on the time period of the comparison, the global emission scenario and the realisation of the climate model run. The bandwidth of the changes is moreover affected by the approach for the calculation of the wave conditions. A significant climate change signal of the average wave conditions is found at westerly wind exposed locations with predominant higher values of the average significant wave heights up to +10%. At easterly wind exposed locations the climate change signal is more weak and higher and lower values are possible (-5% to +5%). Regarding the future changes of the wave directions, in general more wave events from W-NW and fewer events from N-NE can be expected. Analyses of extreme wave heights with a return period of 200 years show both increasing and decreasing values (-0.5m to +0.5m). The climate change signal of the extreme wave events is, as the same for the changes of the average wave conditions, more robust at locations which are exposed to westerly winds.

*Keywords: Baltic Sea, regional climate change, Cosmo-CLM, SWAN wave model, extreme wave conditions*

## INTRODUCTION

The wave climate in the Baltic Sea is very inhomogeneous in space and time, due to the complex topography and the prevailing wind conditions in different parts of the region. Because the local wave climate is mainly generated by the local wind field over the water area, changes of the local wind conditions can directly affect the local wave climate and other local wind driven coastal processes like nearshore currents and the longshore sediment transport. In this study, future wave conditions are presented that provide a basis for the assessment of the effects of regional climate change on the long-term morphological development of the German Baltic Sea coastline. Moreover consequences of climate change on the functional design of coastal protection structures like groins, beach nourishments, breakwaters etc. can be investigated on the basis of the results.

Future projections of the local wave climate can be derived from projections of wind conditions from regional climate model runs. The projections are in general depending on: (i) the atmospheric forcing factors, e.g. the forcing global circulation model, (ii) the global emission scenarios, (iii) the downscaling approach (statistical or dynamical), (iv) the coupling/interaction of the global or regional circulation model with an ocean/sea-ice model and (v) the applied impact model, e.g. a numerical wave model. All these factors result in a large uncertainty of the future projections of wind and waves.

The BACC (2009) report compiles results from different studies on future projections of wind waves in the Baltic Sea, but the results are in general not comparable between the studies due to the specific model set-up used in each of the studies, including different emission scenarios, climate and wave models, downscaling approaches and analysed wave parameters.

In this study dynamical downscaled wind from the regional climate model Cosmo-CLM (Rockel et al., 2008) is used with two realisations each of the IPPC SRES scenarios A1B and B1 (Nakićenović et al., 2000). Cosmo-CLM is forced by the coupled atmosphere-ocean global circulation model ECHAM5/MPI-OM. The wave climate in the area of the Western Baltic Sea is calculated for the past and the future on the basis of the wind data from Cosmo-CLM and the spectral wave model SWAN (Booj et al., 1999).

A recent study on changes of the wave climate in the Baltic Sea, which can be compared for average wave conditions in the deep water to the approach used within this study, is carried out by Groll et al. (2013). In contrast to our study the spectral wave model WAM (Hasselmann et al., 1988) is used for the calculation of the wave conditions in the whole Baltic Sea.

[1] Institute of River and Coastal Engineering, Hamburg University of Technology, Denickestr. 22, Hamburg, 21073, Germany
[2] Chair of Geotechnics and Coastal Engineering, University of Rostock, Justus-von-Liebig Weg 6, Rostock, Mecklenburg-Pommerania, 18059, Germany
[3] Hohai University, 1 Xikang Road, Nanjing, 210098, China

## METHOD

### Wave Model

A wave model for the area of the Western Baltic Sea (model name "WBSSC") is set up on the basis of the 3rd generation spectral wave model SWAN using a high temporal ($\Delta t$=1hour), horizontal ($\Delta x=\Delta y\sim$2km) and directional ($\Delta\Theta$=2.5°) resolution with 42 frequencies ($f_{low}$=0.05Hz, $f_{high}$=1Hz). The local wave model is nested into a coarse wave model ($\Delta t$=1hour, $\Delta x=\Delta y\sim$5.5km, $\Delta\Theta$=15° with 35 frequencies from $f_{low}$=0.04177Hz to $f_{high}$=0.4114Hz) for the whole Baltic Sea. The coarse model is run by the Helmholtz-Zentrum Geesthacht using the wave model WAM (Groll et al., 2013).

For the numerical simulations different boundary conditions are used. The Bathymetry of the coarse and local model is based the topography of the Baltic Sea from Seifert et al. (2001). The Bathymetry of the Western Baltic Sea, which is used for the local model WBSSC, is shown in Figure 1.

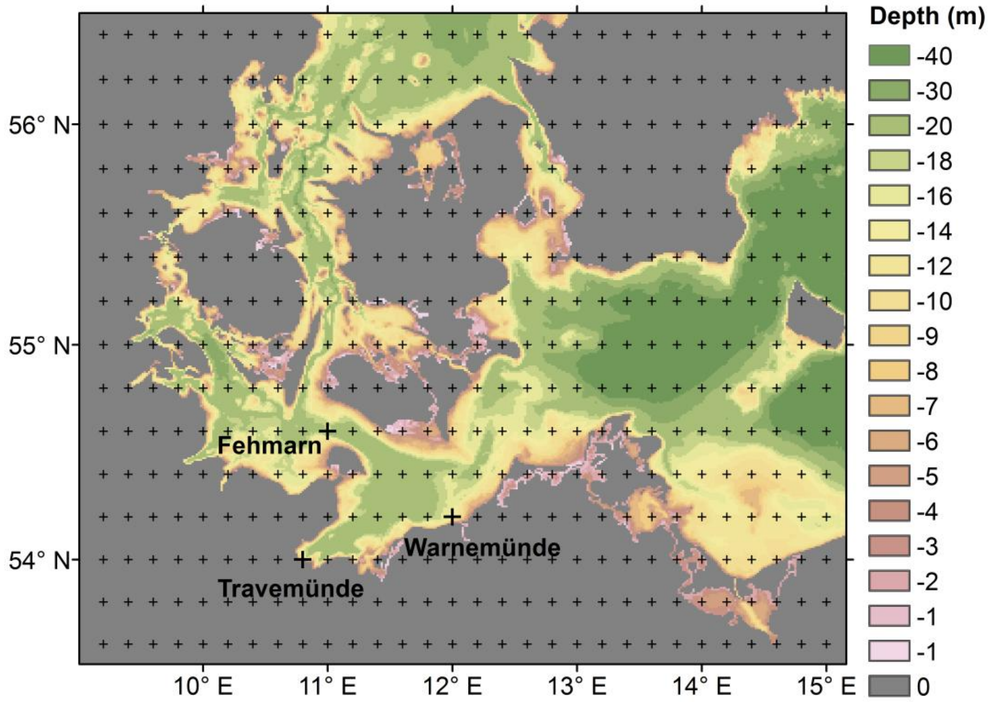


**Figure 1. Bathymetry of the Western Baltic Sea and locations of regular grid points of Cosmo-CLM Datastream 3 (indicated by crosses) and selected locations for the statistical analyses (crosses in bold).**

The exchange of wave information at the northern and eastern boundaries of the local model (SWAN) is done by using hourly wave spectra from the coarse model (WAM). The interpolation to the directions and frequencies of the local model (nested run) is solved by SWAN. For the exchange of the spectral data a free ASCII format (machine independent) is used, including the formatting of the WAM output before it can be proper read into SWAN.

The wind conditions for the local model are used from different runs of the regional circulation model Cosmo-CLM (Lautenschlager et al., 2009). Cosmo-CLM uses dynamical downscaling of the wind data from the forcing global atmosphere-/ocean-ice-model ECHAM5/MPI-OM on the basis of observed anthropogenic emissions resp. the future IPCC emission scenarios (Nakićenović et al., 2000) A1B (global economic) and B1 (global environmental) with two realisations each. The Cosmo-CLM model runs are summarized in Table 1.

**Table 1. Cosmo-CLM model runs and data sets (remark: 'x' denotes no experiment).**

| 20th century (1960-2000) observed anthropogenic forcing | 21st century (2001-2100) forced by emission scenario A1B | 21st century (2001-2100) forced by emission scenario B1 | transient data set (1960-2100) of wind parameter (10m above surface) |
|---|---|---|---|
| C20_1 | A1B_1 | x | C20_1+A1B_1 |
| C20_1 | x | B1_1 | C20_1+B1_1 |
| C20_2 | A1B_2 | x | C20_2+A1B_2 |
| C20_2 | x | B1_2 | C20_2+B1_2 |

The different realisations of the climate model runs represent the climate variability. The realisations of the 20$^{th}$ century (cp. Table 1) are forced by a different realisation of the global ECHAM5/MPI-OM 20C3M simulations (Roeckner et al., 2006a). The global 20C3M simulations are forced with observed natural and anthropogenic emissions at pre-industrial conditions (period about 1860) but are initialised 25 years apart from each other, which ensure the independence of the realisations (Legutke et al., 2009). The global simulations are run for a period from 1860-1955 and are used for the initialisation and forcing of the regional 20C3M simulations. After a 5 years spin-up phase the output of the regional 20C3M simulations is used for the Cosmo-CLM runs for the period 1960-2000. The global 20C3M simulations are continued with the global IPCC emission scenarios A1B and B1 and used for the forcing of Cosmo-CLM between 2001-2100.

In the study we combined the wind data from the Cosmo-CLM model runs for the past and the future to four transient gridded data sets covering a total period from 1960 to 2100 (cp. Table 1).

For the calculation of the wave conditions we used near-surface (10m above surface) hourly wind data from Cosmo-CLM on a regular geographical grid (Datastream 3) with a horizontal resolution of $\Delta x = \Delta y \sim 18$km.

On the basis of the available wind data the wave model is run from the years 1960 to 2100 under sea ice-free conditions and at a mean water level. Since the wave conditions are analysed near the 10m depth contour line ca. 1km off the coast (at quasi deep water conditions) the future sea level rise was neglected for the wave simulations.

## Model Validation

Comparisons between calculated and observed wave parameters were carried out in previous studies (see e.g. Schlamkow, C. & Fröhle, P. 2009). Examples for the comparisons of wave heights and directions near the location of Warnemünde (see Figure 1) are given in Figure 2 resp. Figure 3.

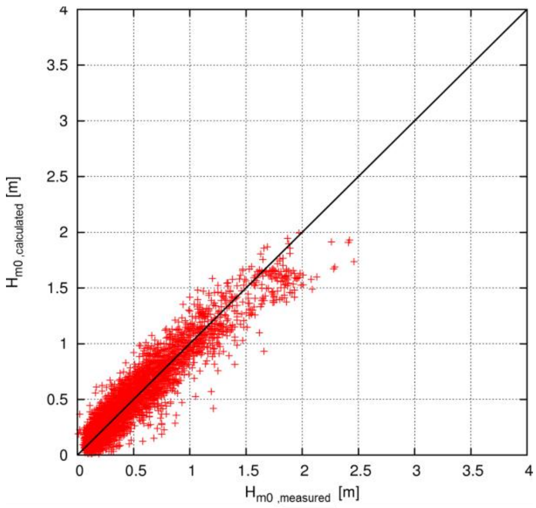


**Figure 2. Calculated (left axis) and observed (bottom axis) significant wave heights (m) near Warnemünde (Schlamkow, C. & Fröhle, P. 2009).**

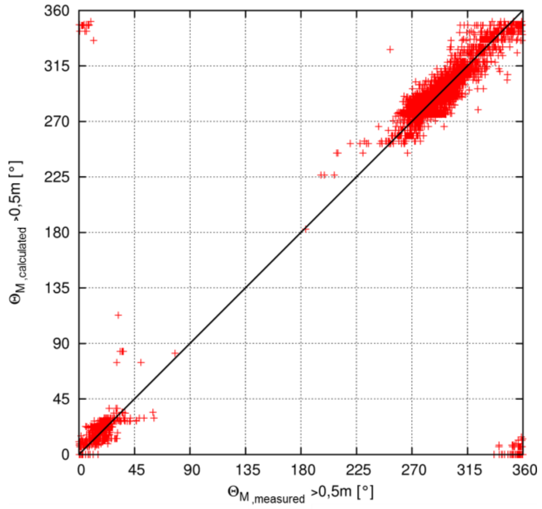


**Figure 3. Calculated (left axis) and observed (bottom axis) mean wave directions (°) for significant wave heights larger than 0.5m near Warnemünde (Schlamkow, C. & Fröhle, P. 2009)**

Figure 2 shows a slight underestimation of higher wave heights due to differences of the input wind field (Local Model of the Deutscher Wetterdienst/DWD) that is used for the calculations. The mean wave directions of significant wave heights larger than 0.5m show a good agreement between observed and calculated values (see Figure 3).

Regarding the mean wave periods a systematic underestimation of the calculated values is found, that is well known from previous simulations (not shown here). For the statistical assessment of the changes of the wave conditions we are focusing on the relative changes of the wave parameters (see next section) and therefore the systematic under- or overestimation of certain wave parameters by the model is neglected.

## RESULTS

### Changes of the average wave conditions

For the assessment of future changes of the wave climate, significant wave heights, mean wave periods and mean wave directions are extracted and averaged for each simulation run (cp. Table 1) over time periods of 30 years, e.g. for the scenarios 2050 (2021-2050) and 2100 (2071 2100) resp. the two control periods 1961-1990 and 1971-2000.

In the next step the relative changes of the wave parameters are calculated between the 30 years average values of the first respectively second realisation of the future scenario runs (A1B_1, B1_1 resp. A1B_2, B1_2) and the 30 years average values of the 20$^{th}$ century runs (C20_1 resp. C20_2).

The relative change of a wave parameter $P$ is defined as

$$\Delta P = \frac{P_{Scenario} - P_{Control}}{P_{Scenario}} \times 100 \qquad (1)$$

where $\Delta P$ is the relative change of the 30 years averages of the wave parameters significant wave height, mean wave period or mean wave direction and the subscripts are denoting the 30 year time periods used for the averages of the wave parameter $P$, e.g. the scenario 2050 (2021-2050) resp. 2100 (2071-2100) and the two control periods 1971-2000 resp. 1961-1990. The relative changes of each wave parameter are calculated for each realisation separately on the basis of annual resp. seasonal averages for winter (DJF), spring (MAM), summer (JJA) and autumn (SON).

**Changes of the 30 years averages of significant wave heights** in the area of the Western Baltic Sea to the end of the 21$^{st}$ century (2071-2100) compared to the control period 1971-2000 for the first realisation of the emission scenario A1B are exemplarily shown in Figure 4.

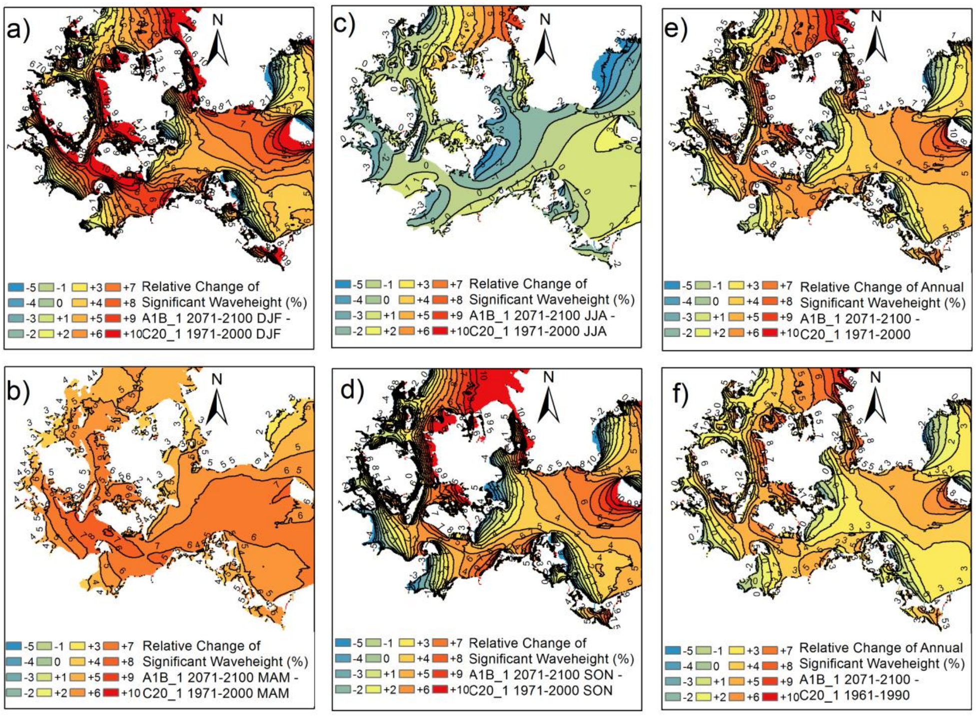


**Figure 4. Relative changes of 30 years SEASONAL averages of significant wave heights during a) winter/DJF, b) spring/MAM, c) summer/JJA, d) autumn/SON for the first realisation of the SRES emission scenario A1B to the end of the 21$^{st}$ century (2071-2100) compared to the values of the control period 1971-2000 and relative changes of 30 years ANNUAL averages of significant wave heights compared to the values of the control period 1971-2000 (e) and 1961-1990 (f).**

As evident from Figure 4 a strong spatial, seasonal and temporal variability of the changes exist. For stretches of the German coastline which are mainly exposed to westerly winds, such as the coastline near Warnemünde or the west coast of the Isle of Fehmarn (cp. Figure 1), predominant higher values of the 30 years averages of the significant wave heights are found. In contrast, at some sheltered locations against westerly winds, such as e.g. the Bays of Lübeck, Kiel or Eckernförde, no change or decreasing values are found.

Moreover the amplitude of the changes is different in each season. At westerly exposed locations, the largest increase of the 30 years averages of the significant wave heights occurs in winter/DJF (cp. Figure 4a). Overall decreases or no changes are evident in summer/JJA (cp. Figure 4c) and overall increases occur especially in spring/MAM (cp. Figure 4b).

Another interesting fact is that the changes of the annual 30 years averages of significant wave heights are different for the chosen control period used for the comparisons. The changes are slightly more pronounced when comparing the future values to the control period 1971-2000 rather than to the control period 1961-1990, which is often used for the assessment of climate change effects in other studies (see e.g. Groll et al., 2013). This phenomenon is the same when the significant wave heights for the scenario 2050 (2021-2050) are compared to the two control periods (cp. Figure 5e and 5f).

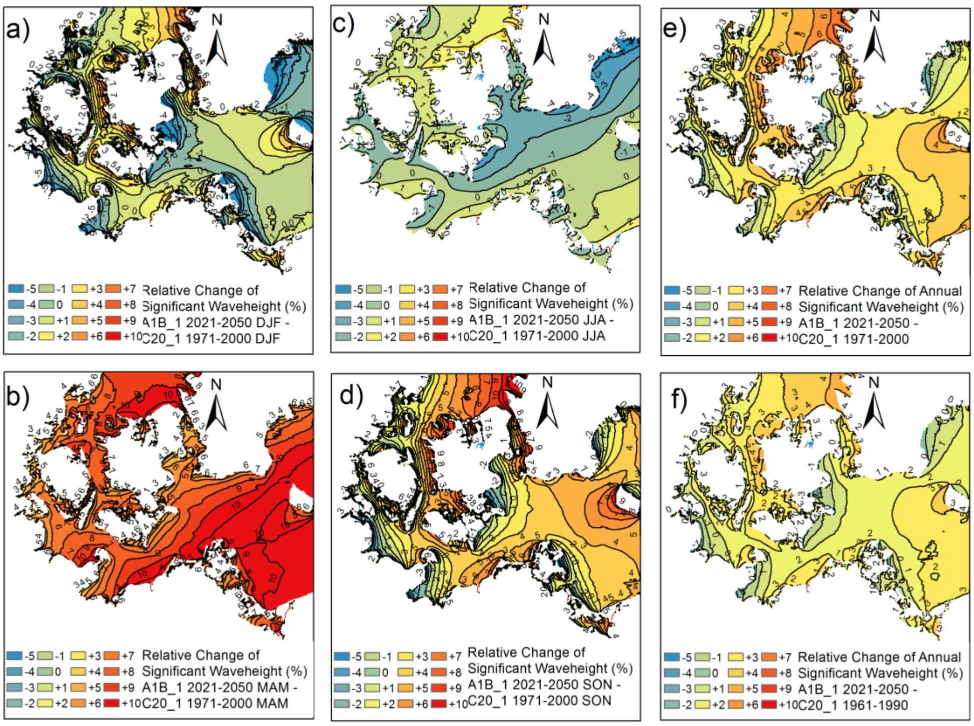


**Figure 5. Relative changes of 30 years SEASONAL averages of significant wave heights during a) winter/DJF, b) spring/MAM, c) summer/JJA, d) autumn/SON for the first realisation of the SRES emission scenario A1B in the middle of the 21st century (2021-2050) compared to the values of the control period 1971-2000 and relative changes of 30 years ANNUAL averages of significant wave heights compared to the values of the control period 1971-2000 (e) and 1961-1990 (f).**

The temporal variability is one of the main influence factors of the amplitude of the changes of the 30 years averages of the significant wave heights. This can exemplarily be seen when comparing the changes in winter/DJF between Figure 4 and Figure 5. While the changes at the end of the 21st century (cp. Figure 4a) are showing larger increases up to +10% at locations which are exposed to westerly winds, slightly lower increasing values are found at the mid-20th century (cp. Figure 5a).

The amplitude of the changes is also different for each realisation of the climate model runs. At the end of the 21st century significant changes at westerly wind exposed locations up to +7% can be found during summer/JJA for the second realisation of the emission scenario A1B (cp. Figure 6c), while for the first realisation the changes are close-to-zero (cp. Figure 4c).

Beside the temporal variability of the changes and the dependency on the realisation of the climate model run, another main influencing factor on the amplitude of the changes is the emission scenario.

An example for this is given from the comparison of the projected changes during winter/DJF and autumn/SON at the end of the 21st century for the first realisations of the emission scenarios A1B (see Figure 4a and 4d) and B1 (see Figure 7a and 7d). For the first realisation of the emission scenario A1B larger increases of the average significant wave heights up to +7% are found during winter/DJF and autumn/SON at locations which are exposed to westerly winds (cp. Figure 4a and 4d), while for the first realisation of the emission scenario B1 the increases during winter/DJF and autumn/SON are much lower.

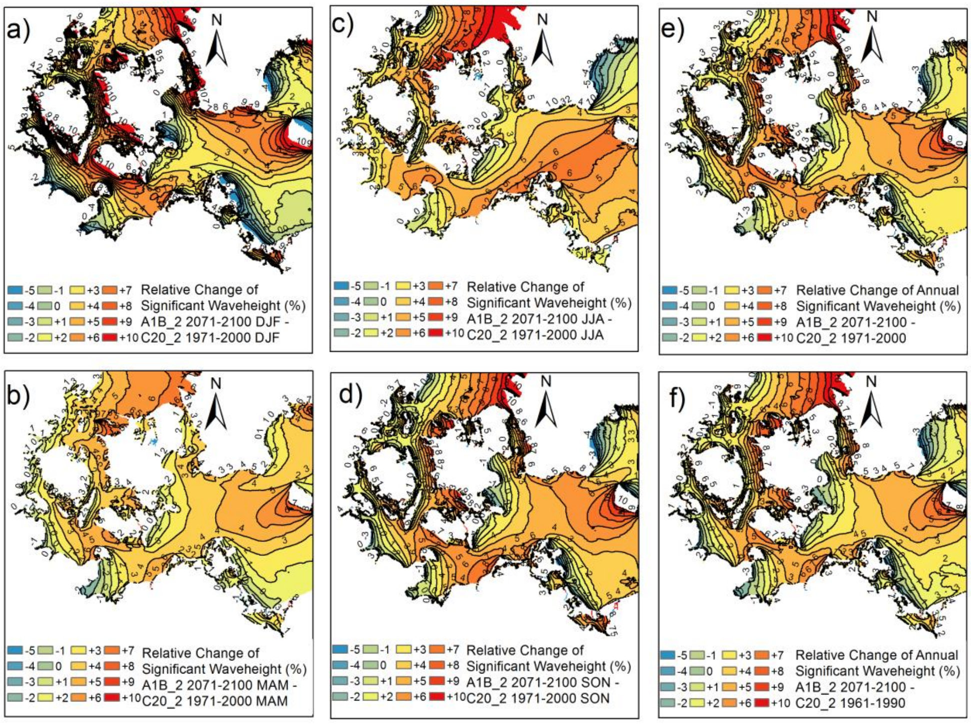


**Figure 6. Relative changes of 30 years SEASONAL averages of significant wave heights during a) winter/DJF, b) spring/MAM, c) summer/JJA, d) autumn/SON for the second realisation of the SRES emission scenario A1B to the end of the 21st century (2071-2100) compared to the values of the control period 1971-2000 and relative changes of 30 years ANNUAL averages of significant wave heights compared to the values of the control period 1971-2000 (e) and 1961-1990 (f).**

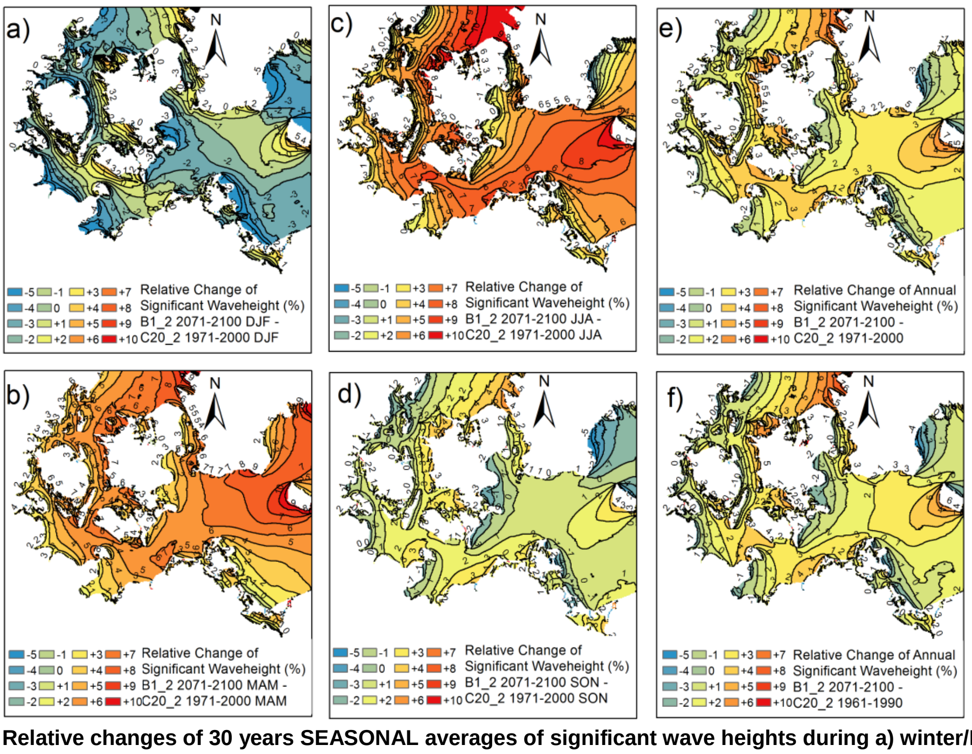


**Figure 7. Relative changes of 30 years SEASONAL averages of significant wave heights during a) winter/DJF, b) spring/MAM, c) summer/JJA, d) autumn/SON for the second realisation of the SRES emission scenario B1 to the end of the 21st century (2071-2100) compared to the values of the control period 1971-2000 and relative changes of 30 years ANNUAL averages of significant wave heights compared to the values of the control period 1971-2000 (e) and 1961-1990 (f).**

**Changes of the 30 years averages of mean wave periods** in the area of the Western Baltic Sea are not as pronounced as for the significant wave heights. The amplitude of the changes of the mean wave periods at westerly wind exposed locations does not exceed +5% (cp. Figure 8d) for first realisation of the emission scenario A1B to the end of the 21st century (2071-2100) compared to the control period 1971-2000.

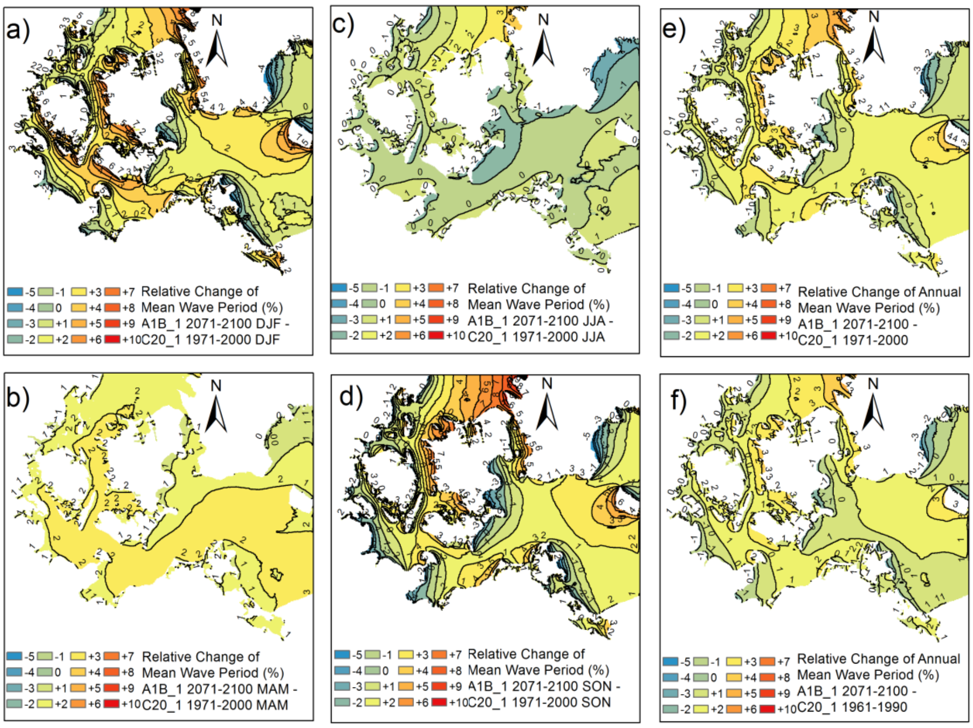


**Figure 8. Relative changes of 30 years SEASONAL averages of mean wave periods during a) winter/DJF, b) spring/MAM, c) summer/JJA, d) autumn/SON for the first realisation of the SRES emission scenario A1B to the end of the 21st century (2071-2100) compared to the values of the control period 1971-2000 and relative changes of 30 years ANNUAL averages of significant wave heights compared to the values of the control period 1971-2000 (e) and 1961-1990 (f).**

**Changes of the 30 years averages of mean wave directions** can have important effects on coastal processes like e.g. the longshore sediment transport at sandy coasts (see e.g. Dreier et al., 2012). The results are not discussed in detail here, but a general trend of the changes of the 30 years annual averages of mean wave direction towards more westerly directions with maximum changes up to 7° at locations which are exposed to westerly winds are found (see Figure 9).

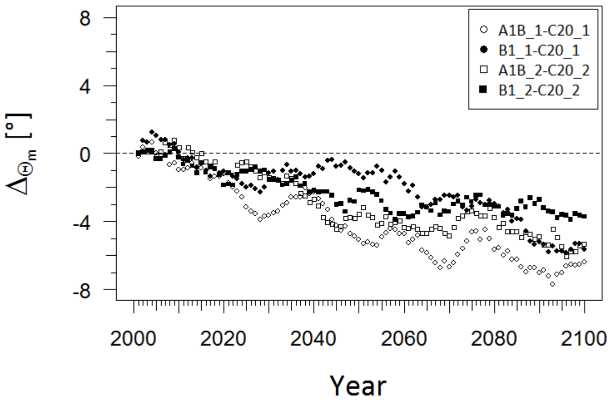


**Figure 9. Relative changes of 30 years annual mean wave direction ($\Delta\Theta_m$) near the location of Warnemünde for the SRES emission scenarios A1B and B1, with two realisations each, compared to the values of the control period 1971-2000.**

**Changes of extreme wave events**

For analysing the changes of extreme wave events we used long-term time series of wave parameters at selected grid points of the Cosmo-CLM model near the locations of Warnemünde, Travemünde and Fehmarn (cp. Figure 1). The time series are analysed with the help of methods of extreme value statistics.

From the time series of significant wave heights we selected samples from time periods of 40 years using the annual maxima (AM) method (see e.g. Coles, S. 2001). After that, different extreme value distribution functions (log-normal, Gumbel, Weibull, GEV) are fitted to the samples and the fitting parameters of the functions are estimated with the help of the maximum-likelihood (MLE) method.

To answer the question which extreme value distribution should be used for the estimation of extreme wave events, a modified Kolmogorov-Smirnov test (Lilliefors test; see e.g. Wilks, D. S. 2011) is applied. For the assessment, difference values like the largest or the root mean square difference between the empirical distribution function (EDF) and the fitted theoretical extreme value distributions EVDs (e.g. log-normal, Gumbel and Weibull distribution) are calculated. Figure 10 shows exemplarily the calculated differences for each EVD of the simulation run B1_1 from 2002-2100 at the selected location near Fehmarn.

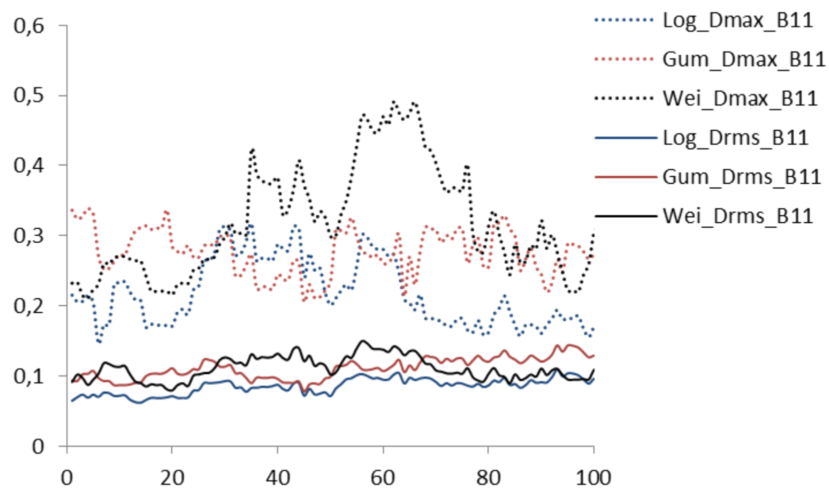


**Figure 10. Maximum differences (dotted lines) and root mean square differences (solid lines) between the empirical distribution of significant wave heights and the theoretical extreme value distribution functions: log-normal (blue), Gumbel (red) and Weibull (black) for the first realisation of the emission scenario B1 near Fehmarn. The x-axis is denoting the number of years within in the future time period from 2001 to 2100.**

In the overall assessment the log-normal extreme value distribution (see blue lines in Figure 10) shows the smallest root mean square differences for most of the simulation runs, thus it is concluded that the log-normal distribution can be regarded as best fitted to the EDF.

On the basis of the log-normal function, the significant wave heights for a chosen return level of 200 years (consecutively called extreme wave heights) are calculated from periods of 40 years of the future (2001-2100) and are compared to the values of the control period 1961-2000 in each simulation run. The relative changes of the extreme wave heights are calculated by using the moving averages method (Eq. 1).

Example results for the relative changes of extreme wave heights at the selected locations (see Figure 1) are shown in Figure 11 for two different approaches for the calculation of the wave heights.

The second approach that we used in previous studies consists of a combined empirical/statistical and numerical approach for the calculation of the wave parameters, consecutively denoted by the acronym "WWC" (for further details see Dreier et al., 2013). The results from the previous study are used to assess the uncertainty of the wave model results.

Figure 11 shows the results from both approaches. The results of the WBSSC wave model in Red are plotted against the results from the WWC approach in Black.

Near Fehmarn (cp. Figure 11 top left) a consistent increasing trend of the changes of the extreme wave heights up to +11% (ca. +0.5m) was found for the simulation runs A1B_2 and B1_2. In contrast, no significant change (WBSSC) respectively a decreasing trend (WWC) was noticed for the simulation run A1B_1. A decreasing trend down to -11% (ca. -0.5m) was found for the simulation run B1_1. Moreover the amplitude of the changes of the extreme wave heights of the emission scenario A1B is lower for the WBSSC approach than for the WWC approach.

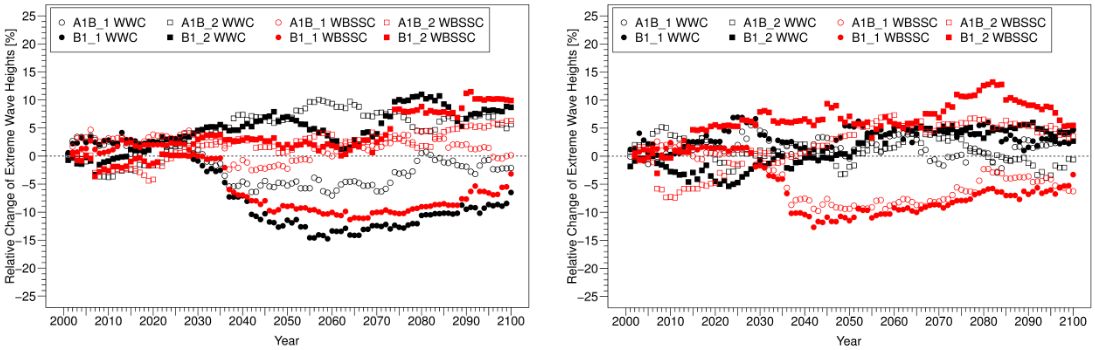


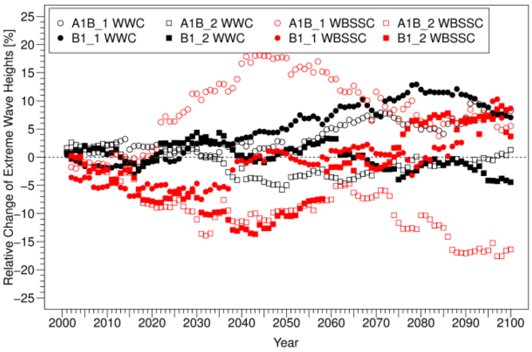


**Figure 11. Changes of significant wave heights with a return level of 200 years (log-normal extreme value distribution function) for simulations runs A1B and B1 compared to the control period (1961-2000) near the locations of Fehmarn (top left), Warnemünde (top right) and Travemünde (bottom left). Results from the numerical simulations are plotted in Red (WBSSC) and results from a combined empirical/statistical-numerical approach are plotted in Black (WWC).**

Near the location of Warnemünde (cp. Figure 11 top right) the same tendencies of the changes as for the location of Fehmarn exist for all simulation runs of the WBSSC approach, except the run A1B_1. Both locations have in common that they are exposed to strong winds from westerly directions. In addition the location near Warnemünde is also exposed to strong winds from north-easterly directions. The bandwidth of changes of the extreme wave heights near Warnemünde ranges between +13% (ca. +0.4m) and -13% (ca. -0.4m) and the uncertainty of the results is larger for the WBSSC approach than for the WWC approach.

The amplitude of the changes of the extreme wave heights near Travemünde (cp. Figure 11 bottom left) strongly depends on the approach used for the calculation of the wave conditions. As for the location of Warnemünde, the bandwidth of results for the WBSSC approach is much larger than for the WWC approach. The extreme wave heights near Travemünde are changing between +18% (ca. +0.3m) and -18% (ca. -0.3m). Moreover the tendencies of the changes are different for each of the simulations runs than compared to the other locations. As an example the strongest increase near Travemünde is noticed for the simulation run A1B_1 while for the other locations the strongest increase occurs for the simulation run B1_2. A possible reason for the different climate change signal is the fact, that the selected location near Travemünde is sheltered against strong winds from westerly directions and mostly exposed by strong winds from north-easterly directions, which might occur less frequent in the future (see also next section of this paper).

## CONCLUSION AND DISCUSSION

Regional climate change can have considerable effects on the wave conditions along the German Baltic Sea Coast. The climate change signal of the wave parameters depends e.g. on: (i) the location resp. the alignment of the coast, (ii) the global emission scenario, (iii) the realisation of the climate model run, (iv) the season, (v) the future time period, (vi) the control period used for the comparison and (vii) the approach used for the calculation of the wave conditions. Because of the manifold drivers of the climate change signal, the uncertainty of the results remains high. Nevertheless some parts of the uncertainty can be addressed by taking into account multi-model ensemble approaches or different realisations of the climate model runs.

Regarding the changes of the **average wave conditions** it can be concluded that increases of the annual and seasonal 30 years averages of the significant wave heights are predominant at coastal stretches which are exposed to westerly winds. The bandwidth of the changes of both annual and seasonal averages of the significant wave heights for the two future scenarios 2050 (2021-2100) and 2100 (2071-2100) compared to actual conditions (1971-2000) ranges between -2% and 10%. Another important fact is that the averages of the mean wave direction change within the range of 3° to 7° towards more westerly wave directions.

At locations which are sheltered against westerly winds (like e.g. the Bays of Lübeck, Kiel and Eckernförde and the East Coasts of the Isles of Fehmarn, Rügen and Usedom) the trend of the changes is unclear and the bandwidth of the changes ranges between -5% to +5%. Minor changes of the averages of mean wave direction within a range of 1° to 2° towards more easterly directions are found.

The changes of the average wave conditions are a result of the changes of the frequency of occurrence of the wave parameters. From previous studies we found at westerly wind exposed locations statistical significant shifts of the frequencies towards higher significant wave heights and more waves coming from westerly directions. In contrast, at locations which are exposed to easterly winds statistical significant shifts of the frequencies towards lower significant wave heights and less waves coming from easterly directions are found. At locations which are exposed to both westerly and easterly winds, both changes of the frequencies of the wave directions are noted.

The changes of the frequencies resp. the averages of the wave parameters can be linked to the changes of the frequencies resp. the averages of the wind velocity and direction. At the selected locations we found in general increases of the 30 years annual averages of the near-surface wind velocities (10m above surface) within a range of +2% to +4% and changes of the 30 years averages of the mean wind direction between 1° and 11° towards more westerly directions to the end of the 21$^{st}$ century (2071-2100) compared with actual conditions (1971-2000). Moreover changes of the frequencies towards higher wind velocities and more wind events from westerly directions are found (for more details see e.g. Dreier et al., 2013).

Regarding the **changes of extreme wave heights**, no robust trend is found until know. Increases and decreases of significant wave heights for return periods of 200 years are found within a range of -18% to +18% (-0.5m to +0.5m). Moreover changes of the return periods of the events can occur.

In the case of an increase of the future extreme wave height, the return period of the event calculated for actual conditions (1961-2000) decreases. In contrast, if the future extreme wave height becomes lower, the return period of the event for actual conditions becomes larger. Nevertheless a high uncertainty of the results is noted, especially regarding the approach which is used for the calculation of the wave conditions.

The results of the changes of the average wave conditions are in good agreement with results from other studies. Groll et al. (2013) use the same global and regional climate model but a different numerical wave model for the calculation of the wave climate (WAM). The changes of the 30 years annual averages of significant wave heights for the first realisation of the emission scenario A1B to the end of the 21$^{st}$ century (2071-2100) compared to the control period 1961-1990 are exemplarily shown in Figure 12. The changes as illustrated in Figure 12 left can be compared to the projected changes of the WBSSC model as shown in Fig 4f.

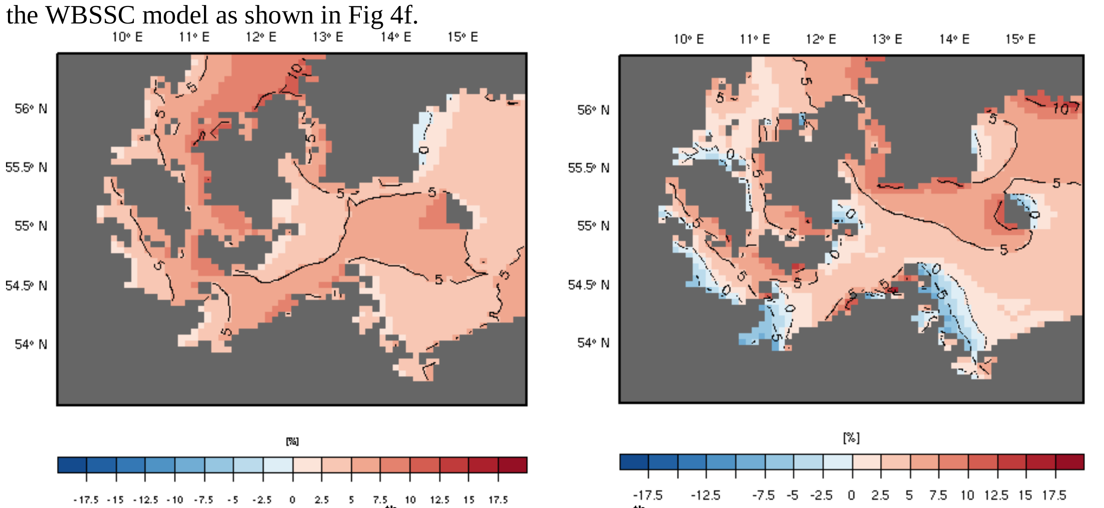


**Figure 12. Relative changes of the 50$^{th}$ percentile (left) and 99$^{th}$ percentile (right) of significant wave heights for the first realisation of the SRES emission scenario A1B to the end of the 21$^{st}$ century (2071-2100) compared to the values of the control period 1961-1990 (from Groll et al., 2013).**

Regarding the changes of higher percentiles of the significant heights Groll et al. (2013) found increases of the 99$^{th}$ percentile of significant wave heights up to +0.5m for the south-eastern part of the Baltic Sea due to changes of the wind conditions over the Baltic Sea (not shown here). The changes of the 99$^{th}$ percentile for the area of the Western Baltic Sea are shown in Figure 12, right. From the results increases of the 99$^{th}$ percentile up to +5% are evident at westerly wind exposed locations and decreases down to -5% are found at sheltered locations against westerly winds.

**ACKNOWLEDGMENTS**

The results described in this publication are achieved within the research project RADOST (Regional Adaptation Strategies for the German Baltic Sea Coast, grant nr. 01LR0807F) as part of the research priority KLIMZUG (Managing Climate Change in Regions for the Future) funded by the German Ministry of Education and Research (BMBF).

**REFERENCES**

BACC. 2008. Assessment of Climate Change for the Baltic Sea Basin. In: Bolle, H.-J., Menenti, M. and Rasool, I. (eds.), Regional Climate Studies, Springer-Verlag Berlin Heidelberg, 2008, ISBN 978-3-540-72785-9. http://www.hzg.de/imperia/md/content/baltex/springer_bacc_complete.pdf

Booij, N., Ris, R.C. and Holthuijsen, L.H. 1999. A third-generation wave model for coastal regions. Part I - Model description and validation. Journal of Geophysical Research, 104, C4, 7649-7666.

Coles, S. 2001. An Introduction to Statistical Modelling of Extreme Values. Springer Series in Statistics. Springer Verlag, London, 2001, p. 208

Dreier, N., Schlamkow, C., Fröhle, P. and Salecker, D. 2013. Changes of 21st Century's average and extreme wave conditions at the German Baltic Sea Coast due to global climate change. In: Conley, D.C., Masselink, G., Russell, P.E. and O'Hare, T.J. (eds.), Proceedings 12th International Coastal Symposium (Plymouth, England), Journal of Coastal Research, Special Issue No. 65, pp. 1921-1926

Groll, N., Hünicke B. and Weisse, R. 2013. Baltic Sea wave conditions under climate change scenarios. In: Reckermann, M. & Köppen, S. (eds.), Conference Proceedings of the 7th Study Conference on BALTEX (10-14 June 2013, Borgholm, Sweden), International BALTEX Secretariat, Publication No. 53, June 2013, p. 62, ISSN 1681-6471.

Hasselmann, S., Hasselmann, K., Bauer, E., Janssen, P.A.E.M., Komen, G.J., Bertotti, L., Lionello, P., Guillaume, A., Cardone, V.C., Greenwood, J.A., Reistad, M., Zambresky, L. and Ewing, J.A. 1988. The WAM model ¬ a third generation ocean wave prediction model. J. Phys. Oceanogr. 18, 1775-1810.

Lautenschlager, M., Keuler, K., Wunram, C., Keup-Thiel, E., Schubert, M., Will, A., Rockel, B. and Boehm, U. 2009. Climate Simulation with COSMO-CLM. Climate of the 20th Century run no.1-3, Scenario A1B run no.1-2, Scenario B1 run no.1-2 , Data Stream 3: European region MPI-M/MaD. World Data Centre for Climate.

Legutke, S., Hollweg, H.-D., Lautenschlager, M., Fast, I., Hennemuth, B., Keup-Thiel, E., Schubert, M. and Wunram, C. 2009. Transient Ensemble Climate Simulations over Europe with the RCM CLM forced by ECHAM5/MPI-OM IPCC AR4 Experiments. Sub. to Meteorologische Zeitschrift. http://www.clm-community.eu/dokumente/upload/f1f46_MetZ_Legutke_et_al_sub_Aug09.pdf

Nakićenović, N., Alcamo, J., Davis, G., de Vries, B., Fenhann, J., Gaffin, S., Gregory, K., Grübler, A., Jung, T.Y., Kram, T., La Rovere, E.L., Michaelis, L., Mori, S., Morita, T., Pepper, W., Pitcher, H., Price, L., Raihi, K., Roehrl, A., Rogner, H.-H., Sankovski, A., Schlesinger, M., Shukla, P., Smith, S., Swart, R., van Rooijen, S., Victor, N. and Dadi, Z. 2000. Emissions Scenarios. A Special Report of Working Group III of the Intergovernmental Panel on Climate Change. Cambridge University Press, Cambridge and New York, pp. 599

Rockel, B., Will, A. and Hense, A. (eds.) 2008. Special Issue: Regional circulation modelling with COSMO-CLM (CCLM). Meteorologische Zeitschrift, Vol. 17.Experimentation. IAHR Design Manual Series, CRC Press/Balkema, Leiden, The Netherlands.

Roeckner, E., Lautenschlager, M., Schneider, H. 2006. IPCC-AR4 MPI-ECHAM5 T63L31 MPI-OM GR1.5L40 20C3M run no.1: atmosphere 6 hour values MPImet/MaD Germany. World Data Center for Climate, doi: 10.1594/WDCC/EH5-T63L31 OM-GR1.5L40 20C 1 6H.

Schlamkow, C. and Fröhle, P. 2009. Entwicklung von Methoden zur Bestimmung maßgebender hydrodynamischer Bemessungsparameter für Küstenschutzanlagen an der Ostsee, Abschlussbericht 3.1 zum KFKI-Verbundprojekt Modellgestützte Untersuchungen zu extremen Sturmflutereignissen an der deutschen Ostseeküste (MUSTOK). Teilvorhaben SEBOK-B. Rostock, 2009, http://edok01.tib.uni-hannover.de/edoks/e01fb09/608411647.pdf

Schlamkow, C. , Dreier, N., Fröhle, P. and Salecker, D. 2012. Future extreme waves at the German Baltic Sea Coast derived from regional climate model runs. Coastal Engineering Proceedings, [S.l.], n. 33, p. management.5, dec. 2012. ISSN 2156-1028. Available at: <https://journals.tdl.org/icce/index.php/icce/article/view/6938>. Date accessed: 26 Aug. 2014. doi:http://dx.doi.org/10.9753/icce.v33.management.5.

Seifert, T., Tauber, F. and Kayser, B. 2001. "A high resolution spherical grid topography of the Baltic Sea – 2nd edition", Baltic Sea Science Congress, Stockholm 25-29. November 2001, Poster #147, www.io-warnemuende.de/iowtopo.

Wilks, D. S. 2011. Statistical methods in the atmospheric sciences. In: Dmowska, R., Hartmann, D. and Rossby, H. T. (eds.), International Geophysics Series, Volume 100, 3rd ed., Academic Press, Elsevier, 2011, 151-154, ISBN 978-0-12-385022-5.